Improving the functional and instantaneous properties of pre-gelatinized riceberry powder through pulsed fluidized-bed agglomeration

Wasan Duangkhamchan[1,2], Sirithon Siriamornpun[3,4]*

[1]Research Unit of Process Design and Automation, Faculty of Engineering, Mahasarakham University, Maha Sarakham, Thailand; [2]Research Unit of Smart Process Design and Automation, Mahasarakham University, Maha Sarakham, Thailand; [3]Research Unit of Thai Food Innovation (TFI), Mahasarakham University, Kantarawichai, Maha Sarakham, Thailand; [4]Department of Food Technology and Nutrition, Faculty of Technology, Mahasarakham University, Kantarawichai, Maha Sarakham, Thailand

***Corresponding Author**: Sirithon Siriamornpun, Research Unit of Thai Food Innovation (TFI), Mahasarakham University, Kantarawichai, Maha Sarakham 44150, Thailand. Email: sirithons@hotmail.com

Academic Editor: Prof. Marco Dalla Rosa – University of Bologna, Italy

Received: 14 December 2024; Accepted: 23 March 2025; Published: 1 July 2025

ORIGINAL PAPER

Abstract

This study investigated the enhancement of the functional properties of pre-gelatinized riceberry powder (PRP) through pulsed fluidized-bed agglomeration using inulin as a binder. Response surface methodology was employed to optimize binder concentration (10–20%) and feed rate (3.5–5.5 mL·min^{-1}) based on key parameters, including final moisture content (6.89–9.46% wb), process yield (71.4–87.2%), and mean particle size (D_{50}, 367–464 µm). The optimal conditions of 20% binder concentration and a 5.5 mL·min^{-1} feed rate resulted in an acceptable moisture content (≤10% wb), a high process yield of 87.2%, and a D_{50} of 464 µm. Agglomeration significantly improved water holding capacity (7.83 g·g^{-1}), oil holding capacity (7.35 g·g^{-1}), and bulk properties such as bulk density, tapped density, particle density, and porosity. These enhancements were attributed to the porous granule structure formed during agglomeration and the amphiphilic nature of inulin, which facilitates hydrophilic and hydrophobic interactions. The combination of inulin and agglomeration also showed potential to moderate the glycemic response while expanding the applicability of PRP in plant-based foods for health-conscious consumers. Despite the powder's high cohesiveness (Carr index 32.5%, Hausner ratio 1.34), it exhibited improved wettability, dispersibility, and reconstitution properties. These findings highlight pulsed fluidized-bed agglomeration with inulin as a promising approach for developing high-performance, plant-based powders for food and beverage applications.

Keywords: air pulsation; instant rice powder; glycemic index; reconstitution; oil holding capacity; water holding capacity

Introduction

The growing demand for convenient and nutritionally enriched products has led to the development of instant powder drinks, valued for their ease of preparation, extended shelf life, and suitability for various dietary needs, particularly among the elderly and individuals requiring specialized nutrition (Zupo *et al*., 2021; Kim *et al*., 2023). These drinks, typically in fine powder form, offer quick rehydration and ease of consumption, addressing challenges related to chewing and digestibility. Among the promising ingredients for such products is

 ISSN 1120-1770 online, DOI 10.15586/ijfs.v37i3.2923

riceberry, a pigmented rice variety native to Thailand. Renowned for its vibrant color and rich nutritional profile, riceberry is packed with antioxidants and bioactive compounds that provide significant health benefits. As a gluten-free, plant-based ingredient, it is particularly well-suited for producing instant powder drinks that cater to health-conscious consumers and those with dietary restrictions (Kongthililerd *et al*., 2020). However, like many fine powders, instant riceberry powder presents challenges such as poor flowability, high cohesiveness, and low solubility, which can impede its processing and reconstitution properties (Rosa *et al*., 2020; Lim *et al*., 2024). Overcoming these limitations requires processing techniques, and pulsed fluidized-bed agglomeration has emerged as a highly effective method. This technique converts fine powders into larger, porous granules, enhancing their flowability, bulk density, and reconstitution properties. The process operates through dynamic and interdependent parameters, including fluidizing air velocity, temperature, binder feed rate, and atomization pressure, all of which influence granule formation and quality. Among these factors, the selection of a suitable binder and its concentration are particularly critical, as they directly affect the binding mechanism, structural integrity, and functional performance of the granules (Nascimento *et al*., 2020; Nascimento *et al*., 2021). Optimizing these parameters is essential for achieving powders that are not only functional but also meet consumer expectations for performance and convenience.

Inulin, a soluble dietary fiber, is gaining attention as a multifunctional binder in agglomeration processes. Its amphiphilic nature, characterized by both hydrophilic and hydrophobic components, enables it to improve water and oil holding capacities, enhance particle binding, and contribute to the formation of stable, porous granules. These properties make inulin a promising candidate for improving the instantaneous and functional attributes of powders. Additionally, inulin contributes to enhanced flowability, reduced cohesiveness, and improved solubility, addressing critical issues in powder handling and performance. Previous studies have demonstrated its success in fluidized-bed agglomeration, where it not only improved functional and handling properties but also added nutritional benefits to powders such as acacia gum (Rosa *et al*., 2020). Despite these advantages, the application of inulin in pulsed fluidized-bed agglomeration, particularly for improving the properties of instant riceberry powder, remains unexplored.

Given the growing demand for high-quality plant-based powders with improved handling and functional properties, this study aims to bridge this gap by utilizing inulin as a binder in pulsed fluidized-bed agglomeration. Specifically, the research focuses on evaluating the effects of varying binder feed rates and concentrations on the agglomeration process and its impact on the quality attributes of pre-gelatinized riceberry powder. Using response surface methodology, the study seeks to identify the optimal agglomeration conditions to enhance key properties, including final moisture content, process yield, and mean particle size. By addressing these challenges, this research aims to advance the development of plant-based instant powders that offer superior functionality, convenience, and consumer appeal.

Materials and Methods

Materials and preparation of pre-gelatinized riceberry powder

Riceberry (*Oryza sativa* L.), as shown in Figure 1A, was traditionally cooked in a domestic electric rice cooker

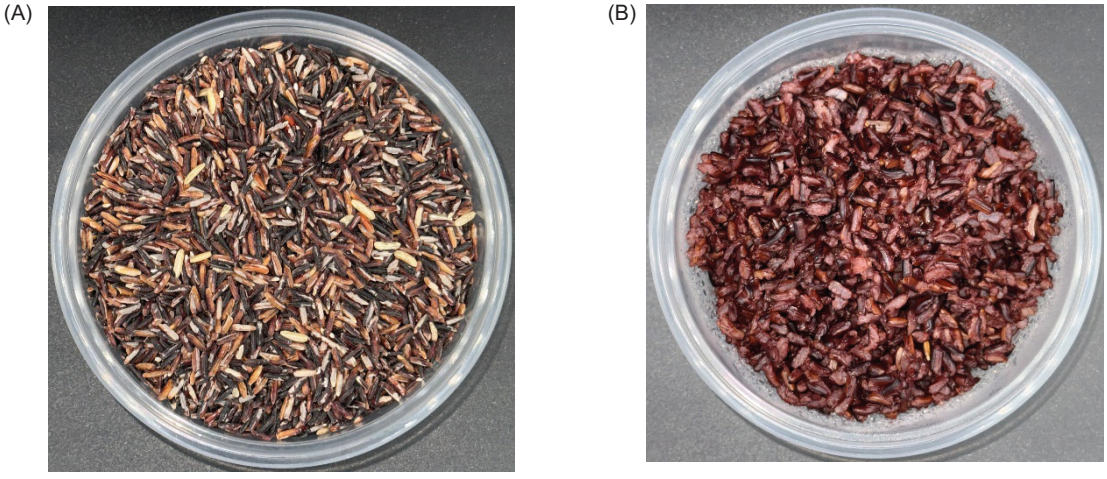

Figure 1. Riceberry (A) and Pre-gelatinized riceberry (B).

with a rice-to-water ratio of 1:3. The pre-gelatinized riceberry (Figure 1B) was then dried in a tray dryer at 60°C until its moisture content dropped below 10% on a wet basis (wb). This pre-gelatinized riceberry was ground and passed through an 80-mesh sieve to produce a fine powder (PRP), which was subsequently stored in an aluminum-foil bag until needed. Additionally, inulin powder, provided by 4Care Co., Ltd., Thailand, was dissolved in distilled water to prepare binder solutions with varying concentrations of 10%, 15%, and 20% by weight.

Experimental setup and agglomeration procedure

Figure 2 illustrates the lab-scale fluidized-bed agglomerator equipped with a pulsed-air setup. Ambient air was drawn into the agglomeration system through an air blower powered by a 1-hp motor (Mitsubishi Electric Automation, Thailand Co., Ltd.) (number 1), with its velocity modulated using an inverter (Model H-3200 Series, Haitec Transmission Equipment Co., Ltd., China) (number 2). The air used for fluidization was heated in a heating box consisting of ten 1-kW finned heaters (number 3), with the temperature regulated by a PID temperature controller (Model MAC-3D, Shimax Co., Ltd., Japan) (number 4).

A fixed sample of 300 g of PRP was introduced into a plexiglass cylinder (number 5) and fluidized at a constant inlet air velocity of 0.5 $m \cdot s^{-1}$ with a fixed temperature of 70°C. To enhance the flowability of the powder, pulsed fluidizing air was introduced through a butterfly valve operated by a DC motor (number 6), with an air pulsation frequency of 0.5 Hz, adjusted using L298N and Raspberry Pi 4B boards. A two-fluid nozzle (number 7), positioned 0.3 m above the air distributor (number 8), was utilized to atomize the binder solution under an atomization pressure of 1 bar. The binder solution was administered via a peristaltic pump (number 9) at varying feed rates of 3.5, 4.5, and 5.5 $mL \cdot min^{-1}$ over a fixed process time of 30 min. During the agglomeration process, elutriated powder was collected using a cyclone (number 10) installed above the reactor. A full factorial experimental design was employed, incorporating two factors at three levels each—binder feed rate (3.5–5.5 $mL \cdot min^{-1}$) and binder concentration (10–20% w/w)—to structure the experimental runs.

Response surface and statistical analysis

Response surface methodology (RSM), associated with a 3^2 full factorial design using Design-Expert (Stat-Ease, Inc.), was used to investigate the impacts of two agglomeration parameters: binder feed rate (3.5–5.5 $mL \cdot min^{-1}$) and binder concentration (10–20% w/w) on the responses of moisture content (MC), mean particle size (D_{50}), and process yield (%yield). Furthermore, quadratic

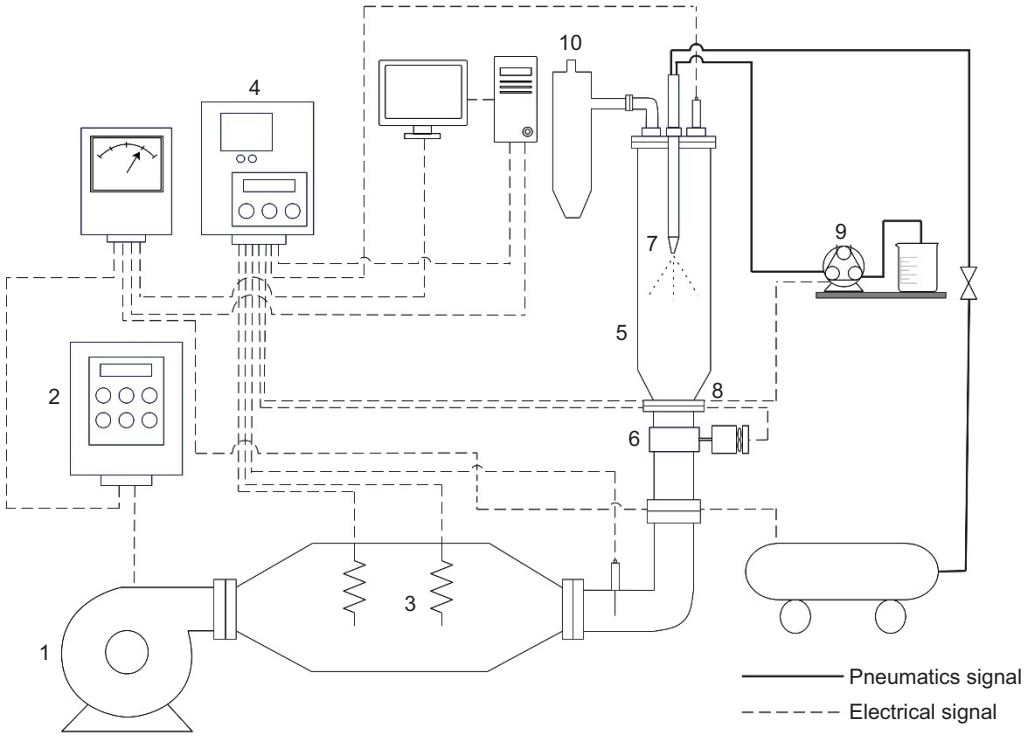

Figure 2. Schematic diagram of a lab-scale fluidized-bed agglomeration system.

correlations of all factors and their responses were used to explore the influence of operating variables on quality attributes.

Mean results were compared using one-way analysis of variance (ANOVA) with Duncan's multiple range test at a 90% confidence level, conducted using SPSS software (IBM Corporation).

Characterization of instant riceberry powder

Moisture content is one of the most important parameters affecting agglomeration efficiency, as it directly impacts bed stability during the process. The moisture content (MC) of powders was determined using a standard oven method (AOAC 2020), which involves briefly drying 3 g of the sample in a hot air oven at 105°C for 48 h. In this work, MC was expressed on a wet basis (wb).

Bulk properties in terms of bulk (ρ_b), tapped density (ρ_t) were determined following the work of Dacanal *et al.* (2016), while particle density (ρ_p) was measured using a gas pycnometer (Ultrapyc 1200e, Quantachrome Instruments, Anton Paar Co., Ltd., Austria) (Jinapong *et al.*, 2008). Powder porosity (ε) was expressed using equation (1).

$$\varepsilon = \left(1 - \frac{\rho_b}{\rho_p}\right) \times 100 \quad (1)$$

Carr Index (CI) representing powder flowability was calculated using equation (2) and used to classify the flowability as follows: CI<15 (very good), 15<CI<20 (good), 20<CI<35 (fair), 35<CI<45 (bad), and CI>45 (very bad) (Dacanal *et al.*, 2016).

$$CI = \frac{\left(\rho_{tap} - \rho_b\right)}{\rho_{tap}} \times 100 \quad (2)$$

Powder cohesiveness was classified using the Hausner ratio (HR), calculated as the ratio of tapped to bulk density (equation 3). Classifications of cohesiveness were as follows: HR<1.2 (low), 1.2<HR<1.4 (intermediate), and HR>1.4 (high) (Dacanal *et al.*, 2016).

$$HR = \frac{\rho_{tap}}{\rho_b} \quad (3)$$

A scanning electron microscope (SEM) (Tabletop Microscope, TM4000Plus, Hitachi, Hitachi High-Tech Ltd.) was utilized to examine the morphology of the particles. The SEM was operated at magnifications of 50× and 100× with an accelerating voltage of 15 kV.

Particle size measurement

Particle size analysis was performed using the laser diffraction method with a particle analyzer (Horiba LA-960V2, Horiba Ltd., Japan), calibrated to a particle refractive index of 1.53. The mean particle size distribution was expressed using the D_{50} values, which represent the diameters below which 50% of the particles fall.

Process yield

Process yield (%yield) was expressed as the powder remaining in the chamber (m_f) after sieving with an 850-µm aperture sieve, avoiding lumps with oversize. The %yield value was calculated using equation (4), where m_i represents the initial powder mass.

$$\%\text{yield} = \frac{m_f}{m_i} \times 100 \quad (4)$$

Reconstitution properties

The protocols proposed by Jinapong *et al.* (Jinapong *et al.*, 2008) were used to determine wettability and dispersibility. Briefly, the wetting time, defined as the time required for 0.1 g of powder to completely sink in 100 mL of water contained in a 250-mL beaker, was determined and expressed as wettability. Dispersibility was measured using the ratio of dissolved powder to the total amount of dry powder, as expressed in equation (5),

$$\%\ \text{dispersibility} = \frac{\left(10 + a\right) \times \%TS}{a \times \frac{100 - b}{100}} \quad (5)$$

where constants a and b represent the mass of the powder used (g) and its moisture content (%wb), respectively, and %TS indicates the dry matter content of the reconstituted powder after sieving.

Water holding and oil holding capacity

Following the methods of Zhou *et al.* (Zhou *et al.*, 2023) and Tian *et al.* (Tian *et al.*, 2024), the water holding capacity (WHC) and oil holding capacity (OHC) of the powder samples were assessed by mixing 0.1 g of the sample with 10 mL of distilled water for WHC or 15 mL of corn oil for OHC. The mixtures were allowed to rest undisturbed at 25°C for 18 h to ensure thorough absorption. After this period, they were centrifuged at 2000 rpm for 15 min. Following centrifugation, the supernatant and any liquid remaining in the tube were carefully removed.

The WHC and OHC values were subsequently calculated using the following equation,

$$\text{WHC (OHC)} = \frac{(M_2 - M_1)}{M_1} \quad (6)$$

where M_1 and M_2 are initial sample and ultimate sample weight (g).

Glycemic index

The predicted glycemic index (pGI) was assessed following the protocols proposed by Goñi *et al.* (1997) and Yusufoğlu *et al.* (2022), using white bread as the reference carbohydrate. A 100 g sample was placed in a centrifuge tube, combined with 10 mL of HCl–KCl buffer (pH 1.5), and vortexed for 15 s. Then, 0.2 mL of pepsin solution (10 mg/mL HCl) was added, and the mixture was incubated at 40°C for 60 min. The volume was adjusted to 25 mL with Tri-maleate buffer (pH 6.9), followed by the addition of 5 mL of α-amylase solution (2.6 IU). Starch hydrolysis proceeded at 37°C, with aliquots taken every 30 min for 180 min to quantify glucose release. Enzyme activity was stopped by heating at 100°C for 15 min and then centrifuged (5000 rpm, 10 min). The supernatant was topped up to 100 mL with 0.1 M sodium acetate buffer (pH 4.5). To complete hydrolysis, 0.1 mL of the solution was mixed with 10 µL of amyloglucosidase and incubated at 50°C for 20 min, followed by the addition of 3 mL of glucose oxidase/peroxidase reagent and another 20-min incubation at 50°C. Glucose was measured at 510 nm using a UV–visible spectrophotometer, converted to starch (by multiplying by 0.9), and expressed as a percentage of total starch hydrolyzed. Samples were analyzed in triplicate.

The pGI was derived from starch hydrolysis kinetics using Equations (7)–(10). In equation (7), C and C_∞ represent the percentages of starch hydrolyzed at each time and at equilibrium, respectively; k is the kinetic constant; and t is time (0–180 min). Equation (8) calculates the area under the curve (AUC), and equation (9) provides the hydrolysis index (HI) by comparing the sample AUC (AUC_s) to the reference AUC (AUC_r). Finally, equation (10) yields the pGI from the HI.

$$C = C_\infty(1 - e^{-kt}) \quad (7)$$

$$AUC = C_\infty\left(t_f - t_0\right) - \left(\frac{C_\infty}{k}\right)\left[1 - e^{-k(t_f - t_0)}\right] \quad (8)$$

$$HI = \left(\frac{AUC_s}{AUC_r}\right) \times 100 \quad (9)$$

$$pGI = 0.7 \times (39.71 + (0.549 \times HI)) \quad (10)$$

Pasting properties

Following Lai (2001) and Yusuf *et al.* (2022), the pasting properties of the powders were determined using a pasting analyzer (RVA4, Newport Scientific, Australia) with a sample suspension of 12% w/v, prepared by mixing 3 g of powder with 25 mL of distilled water. The standard heating method was used to characterize peak viscosity, minimum viscosity, breakdown, final viscosity, setback, and pasting temperature.

Results and Discussion

RSM results and optimal condition

Binder characteristics are crucial factors influencing agglomeration efficiency. In this study, binder concentration and its feed rate were varied to investigate their effects on final moisture content, process yield, and mean particle size using response surface methodology. Table 1 presents the two operating factors, including binder concentration (C) and feed rate (F), along with their responses in terms of final moisture content (MC), process yield (%yield), and mean particle size (D_{50}). The data presented in Table 1 reveal the significant impact of both input parameters on their responses in different ways.

The moisture content of agglomerates is one of the main properties affecting bed stability and the performance of the agglomeration process (Lipps and Sakr 1994; Silva and Taranto 2015; Custodio *et al.*, 2020). In fluidized-bed agglomeration, the binder solution is top-sprayed onto a powder bed, wetting and bridging, followed by drying to form agglomerates. These mechanisms must be balanced to avoid bed collapse and process imperfections. According to Table 1, the un-agglomerated rice powder had a moisture content of 5.91% wb, but this increased to a range of 6.89–9.46% after the agglomeration process under various conditions. These notably higher moisture contents can be attributed to additional moisture retention due to the binder, indicating that binder drying was insufficient for water evaporation during the formation of liquid and later solid bridges (Rosa *et al.*, 2020; Atalar *et al.*, 2021). However, prolonged drying was not necessary, as the moisture contents of the agglomerated powders remained at a safe level, below 10% wb (Quek *et al.*, 2007; Atalar *et al.*, 2021). Nevertheless, the final moisture contents of all agglomerates were within the acceptable safe limit of ≤10% (wb) (Custodio *et al.*, 2020).

Considering the effect of binder feed rate, Table 1 shows that the moisture content of agglomerates increased with an increasing feed rate for all binder concentrations. This positive trend resulted from a higher entry of binder

Table 1. Full factorial experimental runs and their responses.

Operating factor		Response		
C	F	MC	%Yield	D_{50}
10	3.5	7.33±0.79^{bc}	82.76±4.75^{ab}	232.16±1.20^{g}
10	4.5	8.17±0.12^{b}	86.15±2.41^{a}	247.88±1.32^{f}
10	5.5	9.45±0.71^{a}	86.77±1.85^{a}	257.35±0.88^{e}
15	3.5	7.02±0.06^{c}	75.03±6.89^{bcd}	260.11±0.53^{e}
15	4.5	8.19±0.46^{b}	79.70±2.76^{abcd}	263.16±3.07^{e}
15	5.5	9.46±0.82^{a}	82.15±6.35^{ab}	272.16±4.04^{d}
20	3.5	6.89±0.05^{c}	71.86±1.72^{d}	304.66±3.18^{c}
20	4.5	8.04±0.69^{b}	73.37±5.69^{cd}	311.41±3.60^{b}
20	5.5	8.28±0.52^{b}	81.34±5.39^{abc}	463.91±3.56^{a}
Un-agglomerated powder		5.91±0.31^{d}	–	61.47±7.83^{h}

C–binder concentration (% by weight); F–binder feed rate (mL·min^{-1}); MC–moisture content (% wet basis); %yield–process yield (%); D_{50}–mean particle size (μm); Different superscripts represent significantly different value in the same column (p>0.05).

solution into the bed, leading to higher humidity in the wetting-active zone and consequently a lower drying rate under constant input thermal energy. In contrast, an opposite trend was observed despite the increasing binder concentration. This inverse correlation between binder concentration and moisture content at a certain feed rate can be explained by the reduced water content in the binder solution at higher concentrations, which may facilitate faster drying. From these observations, it can be concluded that an optimal balance between binder concentration and feed rate must be considered to achieve high process performance.

The effect of binder concentration and feed rate on the process yield (%yield) of agglomerated pre-gelatinized riceberry powder (PRP) can be observed in Table 1. The results showed that %yields obtained from all experimental runs were higher than 70%, ranging from 71.86% to 86.77%, consistent with the results reported in several studies. Nascimento *et al*. (2020) improved the wettability of pea protein isolate using pulsed fluidized-bed agglomeration with varied binder feed rates of 2.4–3.8 mL·min^{-1}, resulting in process yields of 60–74%. Custodio *et al*. (2020) agglomerated a plant protein blend with a variation in feed rate, ranging from 1.3–2.50 mL·min^{-1}, and reported process yields of 56–82%.

The results in Table 1 show an increasing trend in %yield with a higher feed rate, most evident at 20% binder concentration. Custodio *et al*. (2020) also reported similar results, demonstrating that the high process yield at a high feed rate can be attributed to the increased wetting-active zone, where a larger amount of binder spray is available within the bed for the same agglomeration time, leading to rapid particle growth. The enlarged particles, with lower drag rates, were fluidized with a lower flow, resulting in greater particle retention in the bed. At low feed rates, the increased drying rate due to low humidity in the bed led to a lower process yield. Regardless of the binder feed rate, %yield tended to decrease with higher binder concentration. At low concentration, the higher water content in the binder solution resulted in prolonged drying, promoting more coalescence of wetted particles with a lower drag rate. Elutriation of fine particles was prevented, which consequently provided a higher process yield. These results corresponded to a higher final moisture content of agglomerates when using lower binder concentration. Additionally, the low water level in the binder solution may facilitate a spray-drying effect, where binder droplets dry before depositing onto the particle surface, resulting in imperfections in particle bridging and powder loss. This problematic mechanism is commonly found in a top-spray fluidized-bed configuration (Duangkhamchan *et al*., 2015). The present study revealed that the most efficient agglomeration, in terms of process yield, could be achieved when using a lower binder concentration of 10%.

Mean particle size (D_{50}) is commonly used to evaluate the efficiency of the agglomeration process. As shown in Table 1, the D_{50} of the agglomerates, ranging from 232 μm to 464 μm, was larger than that of the un-agglomerated PRP (~61.47 μm). The impact of agglomeration on particle size was confirmed by SEM micrographs, as shown in Figure 3. SEM micrographs of the un-agglomerated PRP show small, isolated particles with a polysized distribution (Figure 3A, 3B), while the agglomerated powders were noticeably larger with more irregular shapes (Figure 3C–F). The attachment of small particles to form the granules confirmed the agglomeration mechanism. Table 1 shows a positive trend in D_{50} with increasing binder feed rate across binder concentrations. At the highest feed rate of 5.5 mL·min^{-1}, the mean particle size increased most notably under the 20% binder concentration. More binder spray was introduced into the wetting-active zone, resulting in a higher level of humidity in the bed during the same process time. Therefore, the drying rate was lower, allowing more wetted particles to coalesce and form larger granules. A similar trend was observed with variation in binder concentration. This increase in particle size was likely due to the reduction of empty spaces between particles saturated with liquid (Jinapong *et al*., 2008; Custodio *et al*., 2020). The dramatic increase observed at the highest feed rate (5.5 mL·min^{-1}) was attributed to the excessive binder in the bed, which enhanced cohesion and promoted the formation of larger agglomerates.

The ANOVA results summarized in Table 2 highlight the statistical significance of the quadratic relationships,

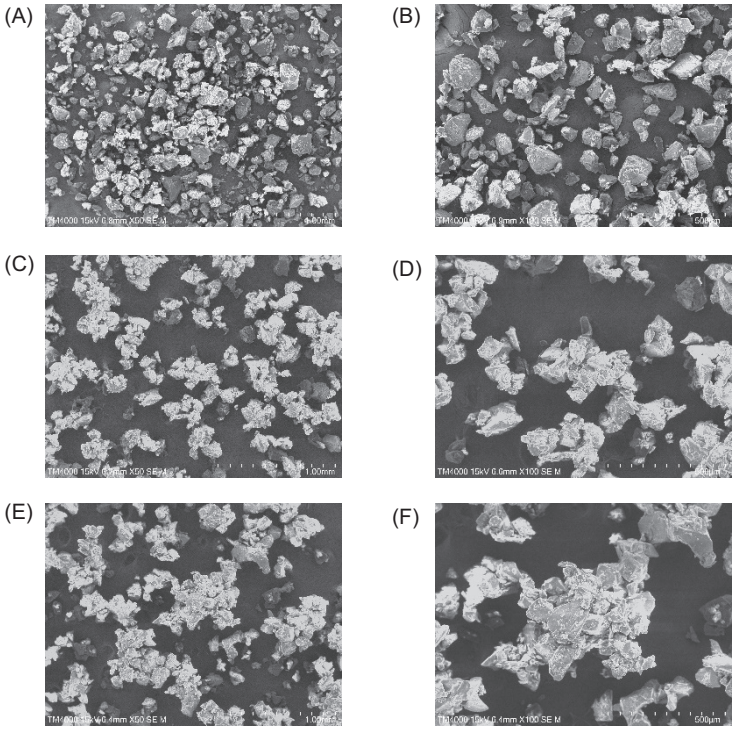

Figure 3. SEM micrographs of un-agglomerated power (A, B), agglomerated under feed rate of 3.5 mL·min−1 and concentration of 10 % (C, D) and feed rate of 5.5 mL·min−1 and concentration of 20 % (E, F) at the magnification of 50x (A, C, E) and 100x (B, D, F).

Table 2. Second-order regression coefficients for moisture content, process yield, and mean particle diameter.

Source	Estimate coefficients		
	MC	%Yield	D_{50}
β_0	8.26	78.80	248.98
β_1	–0.29*	−4.85*	57.10*
β_2	0.99*	3.43*	32.75*
β_{12}	−0.18ns	1.37^{ns}	33.51*
β_{11}	−0.20ns	1.42^{ns}	37.75*
β_{22}	−0.06ns	0.25^{ns}	24.24*
p-value	<0.0001*	0.0006*	<0.0001*
F-value			
Model	12.80	6.87	31.76
X_1	4.88	21.69	90.01
X_2	57.01	10.87	29.61
R^2	0.75	0.62	0.88

*Represents significant difference (p<0.05), while ns stands for 'not significant.'

as expressed in equation (11), between the input variables—binder concentration (C) and feed rate (F)—and the corresponding responses (MC, %yield, and D_{50}). The analysis shows that all models were statistically significant ($p < 0.05$), confirming their reliability in predicting the responses based on the operating parameters investigated in this study.

$$Y = \beta_0 + \beta_1 X_1 + \beta_2 X_2 + \beta_{12} X_1 X_2 + \beta_{11} X_1^2 + \beta_{22} X_2^2 \quad (11)$$

where Y is the estimated response, X_i is the independent process variable and β_i denotes the model coefficient for variable i.

The moisture content model, with an F-value of 12.80 and an R^2 of 0.75, revealed the significance of linear terms, as indicated by a p-value below 0.05. Notably, the binder feed rate (F-value = 57.01) was the most influential factor, followed by binder concentration (F-value = 4.88). These relationships are illustrated in Figure 4, where the highest moisture content (~9.4% wb) occurred at the maximum feed rate (5.5 mL·min^{-1}) and the lowest binder concentration (10%). Conversely, the lowest moisture content (6.9% wb) was observed at 3.5 mL·min^{-1} and 20% binder concentration. The 3-D contour plot (Figure 4) emphasizes that feed rate had a more pronounced effect than binder concentration, with higher feed rates leading to increased moisture due to greater adsorption in the wetting-active zone over the same process duration. This aligns with Custodio *et al*. (2020), who reported similar findings for açaí pulp as a binder. However, higher binder concentrations slightly reduced moisture content, as less water in the binder solution facilitated faster drying, especially

at higher feed rates, as indicated by a negative estimate coefficient (–0.29). Dacanal and Menegalli (2010) also observed a similar trend with maltodextrin concentrations (10–41.9%) for soy protein isolate. Importantly, the influence of binder concentration was more significant at higher feed rates (4.5–5.5 mL·min^{-1}), while at lower feed rates (3.5 mL·min^{-1}), moisture content remained stable despite varying concentrations. These results suggest that optimizing the combination of binder concentration and feed rate is crucial for maintaining desired moisture levels, ensuring bed stability, and achieving optimal granule attributes.

The ANOVA results (Table 2) shed light on the effects of binder concentration and feed rate on process yield (%yield), with the model showing high statistical significance (p = 0.0006, F-value = 6.87), indicating its robustness in capturing the influence of agglomeration parameters. Although the R^2 value (0.62) was relatively low, the model effectively highlighted the stronger impact of binder concentration (F-value = 21.69) compared to feed rate (F-value = 10.87), offering a useful guideline for process control and optimization. Figure 5 illustrates these trends, where the maximum yield (~87%) was achieved at a feed rate of 5.5 mL·min^{-1} and a binder concentration of 10%, while the highest product loss occurred at 3.5 mL·min^{-1} with a concentration of 20%. Increasing binder concentration led to a notable reduction in %yield, particularly at lower feed rates, as reflected by the negative coefficient (–4.85) in Table 2. This reduction is likely due to the lower water content in high-concentration binder solutions, which promotes faster drying and reduces particle coalescence. Consequently, fine particles may exit through the chamber outlet before forming solid bridges, or the binder spray may dry prematurely, causing attrition losses and incomplete solid binding. This adverse trend was not reported by Dacanal and Menegalli (2010), possibly due to the high viscosity of inulin solutions at elevated concentrations, which may produce oversized lumps (>850 µm). Conversely, increasing feed rate consistently improved %yield across all binder concentrations. Higher feed rates expanded the wetting-active zone, enabling more particles to be wetted and promoting rapid particle growth under reduced drying rates. This resulted in larger, heavier granules and minimized process losses caused by fine powder elutriation, as confirmed by the positive coefficient (3.43) for feed rate in the ANOVA analysis (Table 2) and findings from Nascimento *et al*. (2020).

Table 2 highlights a highly significant quadratic relationship for mean particle size (D_{50}), supported by a p-value < 0.0001, an F-value of 32.22, and a robust R^2 value of 0.88, indicating the model's reliability. Notably, all monomial, interaction, and quadratic terms were statistically significant at a confidence level above 95%. Among the factors, binder concentration emerged as the most influential, with an F-value of 91.17, whereas binder feed rate, though significant, had a lesser impact with an F-value of 11.56. As illustrated in the 3D contour plot (Figure 6), the largest agglomerate size was achieved at the highest binder concentration (20%) combined with the maximum feed rate (5.5 mL·min^{-1}), whereas the smallest size occurred at the lowest concentration and feed rate. This increasing trend in particle size with higher binder concentrations aligns with the positive correlation observed in the ANOVA analysis, particularly at high feed rates, which can be attributed to the proportional relationship between the viscosity of the binder solution and the strength of the solid bridges (Lee and Yoo 2023). Similarly, binder feed rate contributed to particle size growth, but its influence was less pronounced at lower

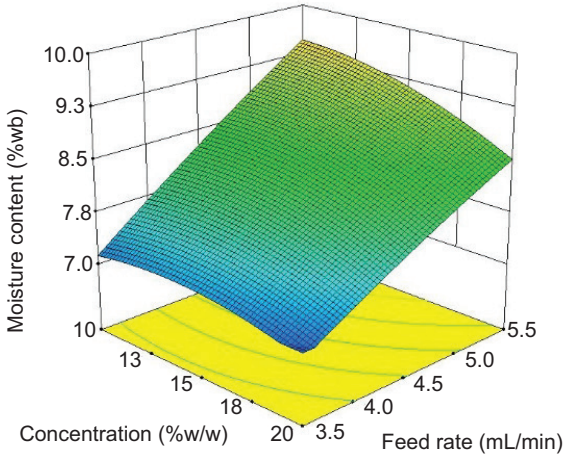

Figure 4. Moisture content of agglomerates as functions of binder concentration and feed.

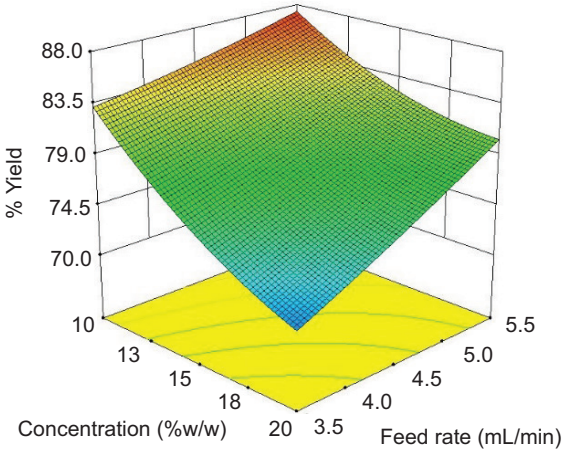

Figure 5. Process yield (%yield) as functions of binder concentration and feed.

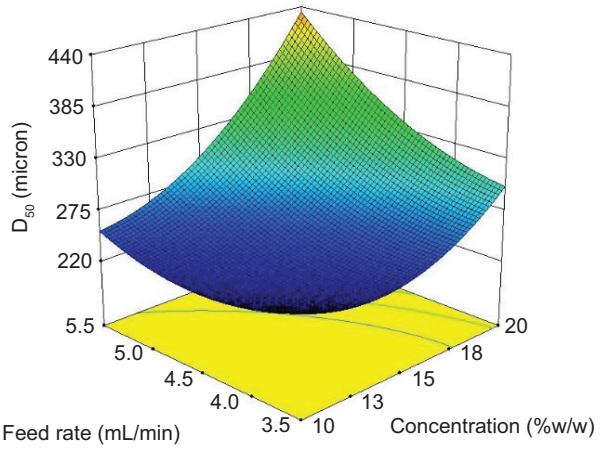

Figure 6. Mean size (D_{50}) of agglomerates as functions of binder concentration and feed rate.

binder concentrations, as evidenced by the profile exhibiting a shallow gradient. At low viscosities, the strength of the solid bridges was insufficient to withstand the forces generated during particle collisions, leading to fracturing as the dominant mechanism (Lee and Yoo 2023). Consequently, these results underscore the need for careful optimization of binder concentration and feed rate to achieve the desired granule size, which is crucial for ensuring the functional properties of the powder.

The optimal operating conditions for the agglomeration process were determined based on key parameters, including final moisture content, process yield, and mean particle size. A binder concentration of 20%, combined with a feed rate of 5.5 mL·min^{-1}, produced the most favorable results, yielding agglomerated powder with an acceptable moisture content (≤10%), a high process yield (~81%), and a median particle size (~464 μm) significantly larger than those obtained under other conditions with similar moisture levels. This optimal combination effectively balanced particle wetting and solid bridging, as indicated by the slight increase in moisture content from the un-agglomerated powder (5.91% wb) to the agglomerates (6.89–9.46% wb). These results highlight the process's ability to maintain stable fluidized bed conditions while minimizing product losses and enhancing the physical attributes of the powder.

While these parameters effectively demonstrate the process efficiency, the functional attributes of the agglomerated powder—affected by feed rate and binder concentration—are equally critical to assess. Since the primary goal of using inulin as a binder was to enhance powder functionality, further analysis is needed to explore these attributes. The following sections will discuss in detail the functional properties of the agglomerates and how they are influenced by the process conditions.

Influence of operating variables on agglomerated powder properties

In addition to the key parameters used to evaluate agglomeration efficiency, such as moisture content, process yield, and particle size, the functional properties of the agglomerated PRP play a crucial role in determining its suitability for practical applications. Bulk properties, flowability, cohesiveness, and reconstitution characteristics are essential attributes that influence powder handling, storage, and performance in end-use scenarios. These properties, summarized in Table 3, are particularly important for ensuring the consistency and quality of the final product—especially when using inulin as a binder to enhance functionality. The following sections will present and discuss these key attributes, including bulk properties, flowability, cohesiveness, reconstitution, and other functional properties, highlighting their dependence on the operating conditions and their implications for the further application of the agglomerated PRP.

Bulk properties

Table 3 highlights the impact of binder feed rate and concentration on the bulk properties, flowability, cohesiveness, and porosity of agglomerated pre-gelatinized riceberry powder (PRP). Significant changes in bulk, tapped, and particle densities, as well as porosity, were observed depending on the operating conditions tested, with agglomerated samples consistently differing from un-agglomerated PRP.

The un-agglomerated powder exhibited a bulk density of 779.61 kg·m^{-3}, which was significantly higher than that of the agglomerates (443.04–510.28 kg·m^{-3}). Similarly, its tapped density (1189.18 kg·m^{-3}) exceeded those of the agglomerates (594.81–750.41 kg·m^{-3}). These decreases in density were most pronounced at the highest binder concentration (20%) and feed rate (5.5 mL·min^{-1}), conditions that also produced the largest granules. This reduction in density is attributed to the formation of larger particles with void structures, leading to less compact agglomerates, as reported by Atalar and Yazici (2019). Both bulk and tapped densities showed a decreasing trend with increasing binder concentration and feed rate, further confirming the impact of these factors on particle compactness.

The particle density of the agglomerates (1513.20–1564.82 kg·m^{-3}) was lower than that of the un-agglomerated PRP (2206.09 kg·m^{-3}), but showed minimal variation across agglomeration conditions. This consistency suggests that the agglomeration process primarily affects the particle's external structure rather than its internal density. Correspondingly, porosity increased

Table 3. Bulk properties, flowability (CI), cohesiveness (HR), and reconstitution properties of PRP.

C	F	Bulk density	Tapped density	Particle density	Porosity	CI	HR	Wetting time	Dispersibility
Binder condition									
10	3.5	510.28±4.62^{b}	750.41±0.27^{b}	1564.82±4.55^{b}	67.39±0.39^{a}	32.00±0.64^{ab}	1.47±0.01^{ab}	52.50±1.27^{b}	47.76±7.00^{f}
10	4.5	498.45±1.40^{bc}	734.17±27.14^{bc}	1563.54±3.96^{b}	68.12±0.17^{de}	32.04±2.70^{ab}	1.47±0.06^{ab}	50.70±1.27^{b}	58.54±0.85^{def}
10	5.5	498.53±8.10^{bc}	719.23±8.54^{bc}	1552.14±4.73^{c}	67.88±0.62^{a}	30.67±1.95^{bc}	1.44±0.04^{bc}	45.30±1.27^{c}	65.46±8.25^{cde}
15	3.5	495.96±6.78^{cd}	711.62±4.37^{cd}	1535.52±4.69^{e}	67.70±0.54^{a}	30.30±1.38^{bc}	1.44±0.03^{bc}	44.40±2.54^{c}	65.22±7.12^{cde}
15	4.5	479.17±5.47^{ef}	685.64±3.06^{d}	1543.28±5.24^{d}	68.95±0.46^{bc}	30.11±1.11^{bc}	1.43±0.02^{bc}	32.40±1.70^{d}	67.83±5.20^{bcd}
15	5.5	484.36±12.95^{de}	682.19±17.37^{d}	1550.54±4.22^{cd}	68.76±0.92^{cd}	29.00±0.09^{bc}	1.41±0.00^{bc}	28.50±0.71^{e}	71.63±1.72^{bc}
20	3.5	464.35±10.63^{g}	641.83±48.52^{e}	1533.02±6.12^{e}	69.71±0.08^{b}	27.46±3.82^{cd}	1.38±0.07^{cd}	23.50±2.12^{f}	73.97±6.96^{bc}
20	4.5	467.77±11.98^{fg}	646.07±38.29^{e}	1513.36±3.88^{f}	69.09±0.21^{bc}	27.50±2.44^{cd}	1.38±0.05^{cd}	25.85±1.63^{ef}	79.64±9.76^{ab}
20	5.5	443.04±11.23^{h}	594.81±8.16^{f}	1513.20±5.05^{f}	70.72±0.84^{a}	25.49±2.91^{d}	1.34±0.05^{d}	16.50±2.12^{g}	89.10±9.57^{a}
Un-agglomerated		779.61±2.88^{a}	1189.18±4.12^{a}	2206.09±9.94^{a}	64.66±0.29^{f}	34.44±0.47^{a}	1.53±0.01^{a}	61.20±2.48^{a}	53.66±2.33^{ef}

C–binder concentration (% by weight); F–binder feed rate (mL·min^{-1}); CI–Carr index; Hausner ratio (HR); Different superscripts represent significantly different value in the same column ($p>0.05$). All densities are expressed in kg·m^{-3}, and porosity in %.

significantly in the agglomerated samples (67.39–70.72%) compared to the un-agglomerated PRP (64%), with the highest porosity observed at the highest binder concentration and feed rate. This increase is attributed to particle enlargement and the formation of voids within the granule structure, as also noted by Atalar *et al*. (2021). Similar trends have been observed in other materials, such as mushroom powder (76%), milk protein isolate powder (72–80%) (Ji *et al*., 2015), and yogurt powder (51–81%) (Atalar and Yazici 2018).

Flowability and cohesiveness, evaluated through the Carr Index (CI) and Hausner Ratio (HR), respectively, showed distinct trends across the tested conditions. The un-agglomerated PRP exhibited a CI value of 34.44%, classifying it as having fair flowability (CI: 20–35%). While the CI values of all agglomerated samples were higher, indicating limited improvement in flowability, cohesiveness showed noticeable enhancements under certain conditions. Specifically, the un-agglomerated PRP, classified as highly cohesive (HR > 1.4), exhibited higher HR values compared to the agglomerated samples. Agglomerates produced with binder concentrations of 10–15% and feed rates of 3.5–5.5 mL·min^{-1} had slightly lower HR values (1.41–1.47), still classified as highly cohesive. Notably, at the highest binder concentration (20%) and feed rate (5.5 mL·min^{-1}), HR values ranged from 1.34 to 1.38, transitioning the powder into the intermediate cohesiveness category (1.2 < HR < 1.4). These results suggest that higher binder concentrations and feed rates reduce cohesiveness while simultaneously improving powder handling properties. The observed trends in CI and HR provide valuable insights for further optimization to enhance both flowability and cohesiveness in agglomerated powders.

Reconstitution properties

This study also examined the effects of binder feed rate and concentration on the wettability and dispersibility of agglomerated powders, as shown in Table 3. Both wettability and dispersibility were generally improved after agglomeration. The process with a feed rate of 5.5 mL·min^{-1} and a binder concentration of 20% resulted in the shortest wetting time of 16.50 s and the highest dispersibility of 89.10%.

Wettability is expressed as the time required to completely wet the powder. As shown in Table 3, the wetting time decreased from 61.20 s to a range of 16.50–52.50 s after agglomeration. The agglomerated powders, which contained more voids, wetted and sank faster into the water, resulting in shorter wetting times. For each binder concentration, a higher feed rate resulted in a shorter wetting time. For instance, at a 15% binder concentration,

the wetting time reduced from 44.40 s at 3.5 mL·min^{-1} to 28.50 s at 5.5 mL·min^{-1}, indicating better wettability. At the highest levels of feed rate and binder concentration, the powder with the largest mean particle size (D_{50} = 464 μm) took the shortest time to become completely wet, while the agglomerates with the smallest size (D_{50} = 232 μm) at a feed rate of 3.5 mL·min^{-1} and a binder concentration of 10% had the longest wetting time, demonstrating that particle enlargement resulted in better wettability. This improved wettability was also reported by Atalar *et al*. (2021), who showed that the wetting time for mushroom powder, overcoming surface tension at the solid-liquid interface, decreased dramatically from several hours to seconds after agglomeration. This enhanced wettability was further confirmed by Atalar and Yazici (2019) and Yuksel and Dirim (2020) for yogurt powder and spinach powder, respectively. Table 3 also shows the adverse effect of binder concentration, with shorter wetting times observed at higher binder concentrations. This is due to the increased void structures inside larger granules, which facilitate faster water penetration. For instance, at a feed rate of 5.5 mL·min^{-1}, the wettability exhibited the following ascending order: 10% (D_{50} = 257 μm), 20% (D_{50} = 272.16 μm), and 30% (D_{50} = 463.91 μm). Additionally, as a soluble fiber, higher inulin concentrations in the binder solution may facilitate easier water absorption during the reconstitution process. This finding was supported by Rosa *et al*. (2020), who demonstrated the improved wettability of acacia gum powder agglomerated with inulin as a binder. The results showed that the agglomerated powder took only 2 s to rapidly sink in the liquid, while the native powder did not even submerge after 600 s.

Dispersibility, which measures the ability of a powder to suspend in an aqueous solution, is one of the critical parameters used to characterize instant powders. Table 3 shows that the dispersibility of agglomerated powders was improved, with values ranging from 47.76% to 89.10%, compared to the un-agglomerated powder (53.66%). The enhanced dispersibility of the agglomerates was linked to their larger size and increased porosity, which facilitated greater liquid penetration. This observation has been reported for various raw materials, such as spinach juice powder (Yuksel and Dirim 2020), pre-gelatinized potato starch powder (Lee and Yoo 2023), xanthan gum powder (Lee and Yoo 2020), and mushroom powder (Atalar *et al*., 2021). Additionally, both binder feed rate and concentration positively impacted the powder dispersibility. For example, at a 10% binder concentration, solubility increased from 47.76% at a 3.5 mL·min^{-1} feed rate to 65.46% at a 5.5 mL·min^{-1} feed rate. This improvement was even more pronounced at higher binder concentrations, with solubility reaching 89.10% at a 20% binder concentration and a 5.5 mL·min^{-1} feed rate. This positive effect can be attributed to the larger voids in the enlarged particles, which facilitate water penetration and increase solubility (Lee and Yoo 2020, Lee and Yoo 2023). Moreover, the higher inulin levels at elevated feed rates and binder concentrations facilitated faster moisture absorption, thus increasing dispersibility (Tsokolar *et al*., 2015). Inulin, known as a soluble fiber, forms a permeable hydrophilic layer, allowing the agglomerated powders to dissolve easily (Ji *et al*., 2016, Lee and Yoo 2023). As a result, higher levels of inulin in the powders at increased feed rates and concentrations can significantly enhance moisture absorption and, consequently, the solubility of the agglomerated riceberry powder.

Water and oil holding capacity and predicted glycemic index

The functional properties of agglomerated pre-gelatinized riceberry powder (PRP), including water holding capacity (WHC), oil holding capacity (OHC), and predicted glycemic index (pGI), offer valuable insights into its suitability for various applications. WHC and OHC reflect the powder's ability to retain water and oil, respectively, which are important for improving texture, stability, and performance in food formulations. Meanwhile, pGI serves as a key indicator of the powder's potential impact on blood glucose levels, which is increasingly relevant with the growing demand for low-glycemic products in health-focused markets. The results of these properties under different binder concentrations and feed rates are summarized in Table 4, and their implications for the

Table 4. Water and Oil holding capacity and predicted glycemic index of PRP agglomerated under different conditions.

Binder condition		WHC	OHC	pGI
C	F			
10	3.5	5.67±0.37^{c}	5.66±0.45^{de}	83.51±0.38^{b}
10	4.5	6.05±0.39^{bc}	5.69±0.31^{e}	82.38±0.36^{b}
10	5.5	6.25±0.04^{b}	5.86±0.19^{de}	83.85±0.65^{b}
15	3.5	6.18±0.20^{bc}	6.04±0.25^{cde}	80.47±0.68^{c}
15	4.5	6.30±0.33^{b}	6.33±0.30^{bcde}	80.33±0.81^{c}
15	5.5	6.56±0.16^{b}	6.55±0.59^{bc}	80.25±0.68^{c}
20	3.5	6.50±0.09^{b}	6.36±0.17^{bcd}	76.51±0.60^{d}
20	4.5	7.49±0.28^{a}	6.91±0.35^{ab}	75.42±0.72^{de}
20	5.5	7.83±0.32^{a}	7.35±0.51^{a}	74.42±0.73^{e}
Un-agglomerated		3.43±0.12^{d}	5.04±0.29^{f}	96.77±2.10^{a}
Raw powder		3.82±0.53^{d}	4.57±0.37^{f}	55.74±0.97^{f}

C–binder concentration (% by weight); F–binder feed rate (mL·min^{-1}); WHC–water holding capacity (g·g^{-1}); OHC–oil holding capacity (g·g^{-1}); pGI–predicted glycemic index; Different superscripts represent significantly different value in the same column (p>0.05).

functional and nutritional qualities of the agglomerates are discussed in detail below.

The WHC values of pre-gelatinized riceberry powder (PRP) significantly increased after the agglomeration process, with values ranging from 5.67 to 7.83 $g \cdot g^{-1}$, compared to 3.82 $g \cdot g^{-1}$ for the raw powder and 3.43 $g \cdot g^{-1}$ for un-agglomerated PRP (Table 4). This improvement can be attributed to two primary factors: the structural changes induced by agglomeration and the amphiphilic nature of inulin. During agglomeration, inulin's hydrophilic properties enhance water retention by forming hydrogen bonds between its hydroxyl (-OH) groups and water molecules. Furthermore, the process creates larger, porous granules with expanded surface areas and increased void spaces, which trap water through capillary action. Higher binder concentrations (20%) and feed rates (5.5 $mL \cdot min^{-1}$) amplified these effects, resulting in the highest WHC values. Additionally, the reduction in bulk density during agglomeration contributed to increased water retention, as more void spaces allowed water to permeate and be absorbed. These results highlight the dual role of inulin and the agglomeration process in improving the hydration properties of PRP, making it highly suitable for applications requiring enhanced water retention, such as in food formulations for improved texture and stability.

The OHC of PRP also demonstrated significant improvements after agglomeration, with values ranging from 5.66 to 7.35 $g \cdot g^{-1}$, compared to 4.57 $g \cdot g^{-1}$ for the raw powder and 5.04 $g \cdot g^{-1}$ for un-agglomerated PRP (Table 4). This enhancement is attributed not only to particle enlargement resulting from agglomeration but also to the amphiphilic nature of inulin, which possesses both hydrophilic and hydrophobic properties. The hydrophobic portion of inulin interacts with water-insoluble components on the rice powder surface, such as fats and starches, forming stronger associations that enhance oil retention. Simultaneously, the structural transformations during agglomeration, such as increased porosity and larger particle sizes, create physical spaces that trap oil through capillary action and mechanical entrapment. Binder concentration played a crucial role, with higher concentrations (20%) yielding the maximum OHC values due to enhanced hydrophobic interactions and more porous granule structures. Similarly, increasing the feed rate promoted uniform binder distribution and robust granule formation, further improving oil retention. These findings emphasize the dual functionality of inulin and its ability to enhance both hydrophilic and hydrophobic interactions, making agglomerated PRP particularly effective in applications such as emulsified foods, where both water and oil retention are essential for product stability and quality.

The predicted glycemic index (pGI) of PRP was significantly reduced following agglomeration, decreasing from 96.77 in the un-agglomerated PRP to a range of 74.42–83.85 in the agglomerated samples (Table 4). Remarkably, increasing levels of inulin were associated with a stepwise reduction in pGI, transitioning from a high glycemic index to a moderate one. This reduction is likely due to the functional role of inulin, which slows carbohydrate digestion and absorption by forming granules that resist enzymatic hydrolysis (Ferreira *et al.*, 2021). Among the agglomeration parameters, binder concentration had the most pronounced effect, as higher inulin levels at 20% concentration led to the lowest pGI values. However, despite this improvement, the agglomerated PRP remains classified as a high-GI product (pGI > 70), indicating that further optimization is needed to achieve a lower glycemic index. Potential strategies include incorporating additional functional ingredients or adjusting formulations to further slow starch digestion. Nevertheless, the combination of inulin and agglomeration has proven effective in moderating glycemic response while simultaneously enhancing other functional properties, such as WHC and OHC. These improvements expand the potential applications of PRP in plant-based foods, especially those targeting consumers seeking healthier, functional food options.

Although these functional changes can influence biological processes such as hydration, nutrient retention, and glycemic response, this study does not directly assess biological properties. Instead, it provides insights into how pulsed fluidized-bed agglomeration alters the physical and chemical characteristics of PRP. These findings lay the groundwork for future studies that could evaluate the biological effects of these modifications in functional food applications.

Pasting properties

The pasting parameters of all samples are illustrated in Table 5. The pasting properties varied significantly among the powder samples. The un-agglomerated powder exhibited a higher pasting temperature compared to the raw sample and had lower viscosity parameters, except for the setback (Table 5). Pre-gelatinization, which results in the degradation of starch granules, was responsible for the lower viscosity against shear stress (Tô *et al.*, 2020).

When using inulin solution as a binder with various feed rates and concentrations, the pasting temperatures were significantly higher than those of the raw and un-agglomerated powders. A similar result was reported by Zhang *et al.* (2019) and Wang *et al.* (2019), who found an increased pasting temperature in sweet potato starch and rice starch, respectively, after being mixed with inulin. All viscosity parameters presented in Table 5 show the adverse effects of binder feed rate and concentration.

Table 5. Pasting properties of PRP agglomerated under different conditions.

Binder condition		Peak viscosity	Minimum viscosity	Breakdown	Final viscosity	Setback	Pasting temperature
C	F						
10	3.5	146.04±0.65^{c}	142.33±0.35^{c}	3.71±0.30^{d}	208.54±2.06^{c}	77.84±0.12^{c}	85.3±0.49^{d}
10	4.5	139.42±1.18^{c}	132.17±2.0^{d}	7.25±0.82^{c}	194.84±3.30^{d}	69.05±1.59^{d}	84.83±1.03^{d}
10	5.5	107.80±0.18^{d}	108.05±0.18^{e}	−0.25±0.35^{e}	156.04±0.06^{e}	57.34±1.89^{e}	87.73±0.53^{c}
15	3.5	101.88±0.64^{de}	101.83±0.35^{ef}	0.04±0.30^{e}	144.37±2.65^{f}	51.75±0.47^{f}	92.58±0.60^{b}
15	4.5	97.96±0.41^{e}	97.83±0.71^{fg}	0.13±0.30^{e}	140.34±0.23^{g}	48.38±1.00^{fg}	94.65±0.00^{a}
15	5.5	95.09±1.89^{e}	95.17±1.89^{fg}	−0.08±0.00^{e}	138.42±2.12^{gh}	48.38±0.06^{fg}	92.98±1.24^{b}
20	3.5	93.00±0.71^{e}	93.04±1.12^{g}	−0.04±0.41^{e}	135.25±0.71^{h}	47.67±0.47^{g}	94.70±0.00^{a}
20	4.5	82.58±0.00^{f}	82.59±0.12^{h}	0.00±0.11^{e}	119.04±0.18^{i}	42.30±1.24^{h}	94.85±1.41^{a}
20	5.5	75.67±0.47^{f}	75.79±0.41^{h}	–0.13±0.06^{e}	110.20±0.53^{j}	39.88±0.42^{h}	95.43±0.04^{a}
Un-agglomerated		169.50±0.11^{b}	158.96±1.12^{b}	10.54±1.01^{b}	252.46±1.47^{b}	93.50±2.59^{a}	82.50±0.14^{e}
Raw powder		216.09±2.35^{a}	177.21±0.76^{a}	38.88±3.12^{a}	259.54±1.00^{a}	82.34±0.23^{b}	72.28±0.60^{f}

C–binder concentration (% by weight); F–binder feed rate (mL·min^{-1}); Different superscripts represent significantly different value in the same column ($p>0.05$).

The decreased peak viscosity of agglomerated powders was attributed to reduced water availability for starch swelling due to the highly hygroscopic nature of inulin, resulting in a lower amount of leached amylose (Zhang *et al*., 2018; Zhang *et al*., 2019). The lower breakdown values suggested that starch granules in the agglomerated powders were more stable during the heating process, indicating an improvement in the heat resistance of starch associated with inulin. This observation was consistent with the results reported by Wang *et al*. (2019), Witczak *et al*. (2014), Ye *et al*. (2018), and Zhang *et al*. (2019). When using inulin as a binder, setback values were lower, as inulin, with its high water-holding ability, enhanced inhibition of the short-term retrogradation of the un-agglomerated powder (Zhang *et al*., 2019).

Conclusions

This study demonstrated the effectiveness of pulsed fluidized-bed agglomeration with inulin as a binder in enhancing the functional and instantaneous properties of pre-gelatinized riceberry powder (PRP). The process significantly improved water holding capacity, oil holding capacity, and bulk properties such as density and porosity, transforming fine powders into larger, porous granules. Additionally, the treatment contributed to better wettability, dispersibility, and reconstitution properties, which are crucial for instant food applications. The study also revealed that the amphiphilic nature of inulin played a critical role in facilitating hydrophilic and hydrophobic interactions, leading to improved hydration and lipid retention properties. Moreover, the combination of agglomeration and inulin moderated the glycemic response, as evidenced by a reduction in the predicted glycemic index, making it a promising approach for the development of functional plant-based powders. The optimal agglomeration conditions—a binder concentration of 20% and a feed rate of 5.5 mL·min^{-1}—yielded granules with desirable moisture content (≤10% wb), high process yield (~81%), and significantly increased particle size (~464 μm), all of which contribute to improved powder handling and performance. However, the study also identified challenges related to flowability and cohesiveness, as the agglomerated PRP exhibited high cohesiveness (Carr index 32.5%, Hausner ratio 1.34).

These findings provide a scientific foundation for the application of pulsed fluidized-bed agglomeration using inulin as a binder in the development of high-performance, plant-based powders. This approach offers potential applications in functional food formulations requiring improved hydration, fat retention, and controlled glycemic response. Future research should focus on optimizing process conditions and exploring innovative strategies to further enhance powder flow properties while maintaining the desired functional characteristics.

Acknowledgements

This research project was financially supported by Thailand Science Research and Innovation (TSRI) and Mahasarakham University.

Data Availability

The datasets generated and/or analyzed during the current study are available from the corresponding author upon reasonable request.

Compliance with Ethics Requirements

This article does not contain any studies with human or animal subjects.

Author Contributions

W.D.: Investigation, Methodology, Formal analysis, Visualization, and Writing-Original draft preparation. S.S.: Conceptualization, Supervision, Project administration, Writing-Review & Editing, and Resource.

Conflict of Interest

The authors declare no conflict of interest.

Funding

This research project was financially supported by Thailand Science Research and Innovation (TSRI).

References

AOAC (2000) *Official methods of analysis of AOAC International* (17th ed.). AOAC International.

Atalar, I., Kurt, A., Sarıcaoglu, F. T., Güld, O., & Gençcelep, H. (2021). Agglomerated mushroom (*Agaricus bisporus*) powder: Optimization of top spray fluidized bed agglomeration conditions. Journal of Food Process Engineering, 44(e13687). https://doi.org/10.1111/jfpe.13687

Atalar, I., & Yazıcı, F. (2018). Influence of top spray fluidized bed agglomeration conditions on the reconstitution property and structure modification of skim yoghurt powder. Journal of Food Processing and Preservation, 42(e13414). https://doi.org/10.1111/jfpp.13414

Atalar, I., & Yazıcı, F. (2019). Effect of different binders on reconstitution behaviors and physical, structural, and morphological properties of fluidized bed agglomerated yoghurt powder. Drying Technology, 37, 1656–1664. https://doi.org/10.1080/07373937.2018.1529038

Custodio, G. R., de Souza, L. F. G., Nitz, M., & Andreola, K. (2020). A protein powder agglomeration process using açaí pulp as the binder: An analysis of the process parameters. Advances in Powder Technology, 31, 3551–3561. https://doi.org/10.1016/j.apt.2020.07.001

Dacanal, G. C., Feltre, G., Thomazi, M. G., & Menegalli, F. C. (2016). Effects of pulsating air flow in fluid bed agglomeration of starch particles. Journal of Food Engineering, 181, 67–83. https://doi.org/10.1016/j.jfoodeng.2016.03.004

Dacanal, G. C., & Menegalli, F. C. (2010). Selection of operational parameters for the production of instant soy protein isolate by pulsed fluid bed agglomeration. Powder Technology, 203, 565–573. https://doi.org/10.1016/j.powtec.2010.06.023

Duangkhamchan, W., Ronsse, F., Siriamornpun, S., & Pieters, J. G. (2015). Numerical study of air humidity and temperature distribution in a top-spray fluidized bed coating process. Journal of Food Engineering, 146, 81–91. https://doi.org/10.1016/j.jfoodeng.2014.09.005

Ferreira, S. M., Capriles, V. D., & Conti-Silva, A. C. (2021). Inulin as an ingredient for improvement of glycemic response and sensory acceptance of breakfast cereals. Food Hydrocolloids, 114, 106582. https://doi.org/10.1016/j.foodhyd.2020.106582

Goñi, I., García-Alonso, A., & Saura-Calixto, F. (1997). A starch hydrolysis procedure to estimate glycemic index. Nutrition Research, 17, 427–437. https://doi.org/10.1016/S0271-5317(97)00010-9

Ji, J., Cronin, K., Fitzpatrick, J., Fenelon, M., & Miao, S. (2015). Effects of fluid bed agglomeration on the structure modification and reconstitution behavior of milk protein isolate powders. Journal of Food Engineering, 167, 175–182. https://doi.org/10.1016/j.jfoodeng.2015.01.012

Ji, J., Fitzpatrick, J., Cronin, K., Maguire, P., Zhang, H., & Miao, S. (2016). Rehydration behaviors of high protein dairy powders: The influence of agglomeration on wettability, dispersibility, and solubility. Food Hydrocolloids, 58, 194–203. https://doi.org/10.1016/j.foodhyd.2016.02.030

Jinapong, N., Suphantharika, M., & Jamnong, P. (2008). Production of instant soymilk powders by ultrafiltration, spray drying, and fluidized bed agglomeration. Journal of Food Engineering, 84, 194–205. https://doi.org/10.1016/j.jfoodeng.2007.04.032

Kim, S., Kwon, Y. S., & Hong, K. H. (2023). What is the relationship between the chewing ability and nutritional status of the elderly in Korea? Nutrients, 15, 2042. https://doi.org/10.3390/nu15092042

Kongthililerd, P., Suantawee, T., Cheng, H., Thilavech, T., Marnpae, M., & Adisakwattana, S. (2020). Anthocyanin-enriched riceberry rice extract inhibits cell proliferation and adipogenesis in 3T3-L1 preadipocytes by downregulating adipogenic transcription factors and their targeting genes. Nutrients, 12, 2480. https://doi.org/10.3390/nu12082480

Lai, H.-M. (2001). Effects of hydrothermal treatment on the physicochemical properties of pregelatinized rice flour. Food Chemistry, 72, 455–463. https://doi.org/10.1016/S0308-8146(00)00261-2

Lee, H., & Yoo, B. (2020). Agglomerated xanthan gum powder used as a food thickener: Effect of sugar binders on physical, microstructural, and rheological properties. Powder Technology, 362, 301–306. https://doi.org/10.1016/j.powtec.2019.11.124

Lee, H., & Yoo, B. (2023). Particle agglomeration and properties of pregelatinized potato starch powder. Gels, 9, 93. https://doi.org/10.3390/gels9020093

Lim, W., Jeong, Y., Lee, W., & Yoo, B. (2024). Improved physical and structural properties of high-protein powders by fluidized-bed

agglomeration. Food Biotechnology, 33, 1407–1412. https://doi.org/10.1007/s10068-023-01447-2

Lipps, D. M., & Sakr, A. M. (1994). Characterization of wet granulation process parameters using response surface methodology. 1. Top-spray fluidized bed. Journal of Pharmaceutical Sciences, 83, 937–947. https://doi.org/10.1002/jps.2600830705

Nascimento, R. F., Rosa, J. G., Ávila, M. F., & Taranto, O. P. (2021). Pea protein isolate fluid dynamics and characterization obtained by agglomeration in pulsed fluidized bed. Particulate Science and Technology, 39, 809–819. https://doi.org/10.1080/02726351.2020.1830209

Nascimento, R. V., Rosa, J. G., Andreola, K., & Taranto, O. P. (2020). Wettability improvement of pea protein isolate agglomerated in pulsed fluid bed. Particulate Science and Technology, 38, 511–521. https://doi.org/10.1080/02726351.2019.1574940

Quek, S. Y., Chok, N. K., & Swedlund, P. (2007). The physicochemical properties of spray-dried watermelon powders. Chemical Engineering and Processing, 46, 386–392. https://doi.org/10.1016/j.cep.2006.06.020

Rosa, J., Nascimento, R. F., Andreola, K., & Taranto, O. (2020). Acacia gum fluidized bed agglomeration: Use of inulin as a binder and process parameters analysis. Journal of Food Processing Engineering, 43, e13409. https://doi.org/10.1111/jfpe.13409

Silva, C. A. M., & Taranto, O. P. (2015). Real-time monitoring of gas-solid fluidized-bed granulation and coating process: Evolution of particle size, fluidization regime transitions, and psychometric parameters. Drying Technology, 33, 1929–1948. https://doi.org/10.1080/07373937.2015.1076000

Tian, X.-Y., Liu, J.-F., Qiao, C.-C., Cheng, Z., Wu, N.-N., & Tan, B. (2024). Functional properties and structure of soluble dietary fiber obtained from rice bran with steam explosion treatment. Journal of Cereal Science, 118, 103938. https://doi.org/10.1016/j.jcs.2024.103938

Tô, H. T., Karrila, S. L., Nga, L. H., & Karrila, T. T. (2020). Effect of blending and pregelatinizing order on properties of pregelatinized starch from rice and cassava. Food Research, 4, 102–112. https://doi.org/10.26656/fr.2017.4(1).245

Tsokolar-Tsilopoulos, K. C., Katsavou, I. D., & Krokida, M. K. (2015). The effect of inulin addition on structural and textural properties of extruded products under several extrusion conditions. Journal of Food Science and Technology, 52, 6170–6181. https://doi.org/10.1007/s13197-015-1718-2

Wang, R., Wan, L., Liu, C., Xia, X., & Ding, Y. (2019). Pasting, thermal and rheological properties of rice starch partially replaced by inulin with different degrees of polymerization. Food Hydrocolloids, 92, 228–232. https://doi.org/10.1016/j.foodhyd.2019.02.008

Witczak, T., Witczak, M., & Ziobro, R. (2014). Effect of inulin and pectin on rheological and thermal properties of potato starch paste and gel. Journal of Food Engineering, 124, 72–79. https://doi.org/10.1016/j.jfoodeng.2013.10.005

Ye, J., Yang, R., Liu, C., Luo, S., Chen, J., Hu, X., & Wu, J. (2018). Improvement in freeze-thaw stability of rice starch gel by inulin and its mechanism. Food Chemistry, 268, 324–333. https://doi.org/10.1016/j.foodchem.2018.06.086

Yuksel, H., & Dirim, S. N. (2020). Application of the agglomeration process on spinach juice powders obtained using spray drying method. Drying Technology, 39, 19–34. https://doi.org/10.1080/07373937.2020.1832515

Yusuf, M. T. O., Masahid, A. D., Ratnawati, L., Indrianti, N., Ekafitri, R., Sholichah, E., Afifah, N., Sarifudin, A., Hikal, D. M., Sami, R., Khojah, E., Aljahani, A. H., Al-Moalem, M. H., & Fikry, M. (2022). Impact of heating temperature on the crystallization, structure, pasting, and hydration properties of pre-gelatinized adlay flour and its implementation in instant porridge product. Crystals, 12(5), 689. https://doi.org/10.3390/cryst12050689

Yusufoğlu, B., Yaman, M., & Karakus, E. (2022). Glycemic evaluation of some breads from different countries via in vitro gastrointestinal enzymatic hydrolysis system. Food Science and Technology, 42, 334920. https://doi.org/10.1590/fst.34920

Zhang, B., Bai, B., Pan, Y., Li, X. M., Cheng, J. S., & Chen, H. Q. (2018). Effects of pectin with different molecular weight on gelatinization behavior, textural properties, retrogradation, and in vitro digestibility of corn starch. Food Chemistry, 264, 58–63. https://doi.org/10.1016/j.foodchem.2018.05.011

Zhang, L., Wang, X., Li, S., Sun, J., & Liu, X. (2019). Effect of inulin on the pasting, textural, and rheological properties of sweet potato starch. CyTA – Journal of Food, 17, 733–743. https://doi.org/10.1080/19476337.2019.1645738

Zhang, L., Wang, X., Li, S., Sun, J., & Liu, X. (2019). Effect of inulin on the pasting, textural, and rheological properties of sweet potato starch. CyTA – Journal of Food, 17, 733–743. https://doi.org/10.1080/19476337.2019.1645738

Zhou, L. L., Luo, J. Q., Xie, Q. T., Huang, L. H., Shen, D., & Li, G. Y. (2023). Dietary fiber from navel orange peel prepared by enzymatic and ultrasound-assisted deep eutectic solvents: Physicochemical and prebiotic properties. Foods, 12(10), 2007. https://doi.org/10.3390/foods12102007

Zupo, R., Castellana, F., De Nucci, S., Dibello, V., Lozupone, M., Giannelli, G., De Pergola, G., Panza, F., Sardone, R., & Boeing, H. (2021). Beverage consumption and oral health in the aging population: A systematic review. Frontiers in Nutrition, 8, 762383. https://doi.org/10.3389/fnut.2021.762383